NLTE modeling of lines in expanding shells of LPVs

U. Bolick, He. Richter and E. Sedlmayr

(Zentrum für Astronomie und Astrophysik, TU Berlin, D-10623 Berlin, Germany)

Correspondence to: bolick@astro.physik.tu-berlin.de or richter@astro.physik.tu-berlin.de

1 Introduction

The dynamics of the cool, shock penetrated, expanding atmospheres of Long Period Variables (LPVs) can be studied by spectral lines of various atoms or molecules. Especially the infrared molecular line profiles of the CO molecule are excellent diagnostic tools appropriate for the overall structure of the inner, expanding circumstellar layers. Due to the high abundance of CO as well as its formation and stability at high temperatures it is dominant in the circumstellar shells of LPVs. If one focuses on the detailed shock structures in atmospheric layers close to the photosphere for example, various optical atomic lines of neutral and ionized metals (e.g. Mg I, Fe I, Fe II) are suitable diagnostic tools (see Richter & Wood 2001).

To model the various atomic and molecular lines of interest, a radiative transfer code (time-independent, spherical symmetric, co-moving frame, accelerated lambda iteration) has been developed to handle the especially awkward conditions of cool LPV's atmospheres. Here we present and discuss in detail results of infrared CO-line calculations and give a brief outlook on work in progress for optical metal line calculations.

2 About the code

The code is designed to solve the NLTE radiative transfer problem under the especially awkward conditions of cool, pulsating LPV atmospheres. All molecular or atomic lines of interest are calculated by:

- **Radiative transfer:** time-independent, spherical symmetric, co-moving frame (CMF) (Mihalas et al. 1975)
- **Numerical approach:** Feautrier method, 2nd & 1st order discretization (Richtmyer & Morton 1967)
- **Rate equation-system:** Solved with gauss-solver and adjusted, damped newton iteration
- **NLTE iteration:** by accelerated lambda operator (ALO) (Puls 1991; Rybicki & Hummer 1991)
- **Hydrodynamical input models:** snapshots of time-dependent models of shocked, dust-forming, expanding atmospheres (Fleischer et al. 1992, Winters et al. 2000a), radiative transfer and hydrodynamic models *not* coupled

3 Test of the CMF-solution

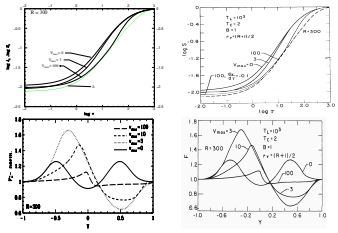

Fig. 1: Isothermal model atmosphere with outer boundary R=300 R_*, different velocities v_{max}, norm. thermalization parameter ϵ=$2 \cdot 10^{-3}$, and total optical depth in the line T_l and continuum T_c. **Upper Left:** Line source function S_l and the mean intensity of the continuum J_c (green triangles). **Upper right:** Results of Mihalas et al. 1975 for the same model atmosphere shown for comparison. **Lower left:** Resulting fluxes of our code in units of continuum versus displacement from the line center Y=x/x_{max}. **Lower right:** Corresponding flux results of Mihalas et al. 1975.

To test the solution of the radiative transfer in the co-moving frame a 2-level-atom was computed for isothermal model atmospheres according to Mihalas et al. 1975 by Richter 1998. In this special case the *coupled* system of rate equation and radiative transfer must not be solved, because the rate equation is included in the line source function. Consequently, one can simply adjust LTE or NLTE using a normalized thermalization parameter ϵ. The hydrodynamical input for the test calculation is given by simple analytic functions: the wind profile is an arctan-function with maximal wind velocity v_{max} at outer boundary R, the absorption coefficients for line and continuum are proportional to the density.

Fig. 1 shows the results for one of the calculated models, namely the R=300 R_* model. One can see the very good agreement between our results computed with accelerated lambda approximation (Puls & Herrero 1988, Puls 1991) and the results of Mihalas et al. 1975 obtained with elimination scheme (Rybicki 1971). This demonstrates that the code solves the radiative transfer in the co-moving frame satisfactory. The resulting line fluxes are depicted in the lower part of Fig. 1 in comparison to the results of Mihalas et al. 1975. The results of our flux calculations are also adequate.

4 LPV-models

As already noted above the complex atmospheric structures characterized by e.g. strong shock waves used as input for our calculations are the result of fully self-consistent model calculations of circumstellar dust shells (CDS) around LPVs, which are described in Fleischer et al. 1992 and Winters et al. 2000a.

For our radiative transfer calculations we have chosen two hydrodynamical input models, which differ only by one input parameter, namely the initial temperature T_0. However the resulting hydrodynamical structures appear to be very similar (see Figs. 5, 6 left panels).

Tab. 1: Parameters of the hydrodynamical input models

Model	M_* [$M_\odot$]	L_0 [$L_\odot$]	T_0 [K]	ϵ_C/ϵ_O	P [d]	Δu_p [km/s]	$<\dot{M}>$ $M_\odot$/yr	$<v_\infty>$ [km/s]
W69	1.0	$1.0\,10^4$	2800	1.30	640	5	$1.7\,10^{-5}$	13.1
W64	1.0	$1.0\,10^4$	2600	1.30	640	5	$3.4\,10^{-5}$	12.6

Model parameters: mass M_*, initial luminosity L_0 and effective temperature T_0, element abundance ε_i (i: carbon, oxygen), period P and velocity amplitude of piston motion Δu_P. **Resulting values:** average mass loss rate $<\dot{M}>$ and final outflow velocity $<v_\infty>$.

5 Modeling of CO-lines

Our CO-model-molecule consists of 3 vibrational bands v=0, 1 and 2 which include 30 rotational levels each. The required CO-data (e.g. energy levels and Einstein coefficients) are calculated according to Chackerian & Tipping 1983, besides the collision rates for H_2-CO collisions which were kindly provided by the group of Prof. W.H. Kegel, Uni Frankfurt. Based on the LPV-models all possible rotational-vibrational CO line profiles for the vibrational transitions v 0−1 (fundamental), v 0−2 (first overtone), and v 1−2 are calculated assuming NLTE for *all* levels. Here we discuss the results of selected rotational transitions of the R-branch: R1, R14, and R25.

The aim of the CO-studies is to show in principal which parts of the hydrodynamical model atmospheres lead to deviations from LTE in the line calculations and to analyze whether the lines actually form in these regions (Sec. 5.1 and 5.2). Furthermore, we want to get an insight on how the rather complex hydrodynamical structures protrudes in rotational-vibrational CO line profiles (Sec. 5.3).

5.1 Deviation from LTE

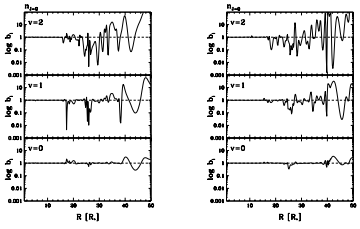

Fig. 2: b-factors versus radius for vibrational bands v = 0, 1, 2 and rotational level J = 0 for calculations with input models W64 (left) and W69 (right).

To demonstrate in which parts of the atmosphere the level population of the 3 vibrational CO-bands deviates from LTE the corresponding b-factors are studied, which are defined by $b_i = n_{i,\mathrm{NLTE}}/n_{i,\mathrm{LTE}}$ for each rotational-vibrational level i. Fig. 2 depicts the b-factors for the rotational level $J = 0$ of all 3 vibrational bands. It can be seen that for both input models the resulting b-factors are of the order of 1 in the inner parts of the circumstellar shell, hence these regions are in LTE. However, the b-factors start to depart significantly from LTE for $r \geq 25$ R$_*$ (v=0) and $r \geq 18$ R$_*$ (v=1, v=2) for model W69 whereas model W64 shows strong deviations already for $r \geq 18$ R$_*$ in all bands. One can therefore conclude that no NLTE effects occur in model W69 if the v 0−1 lines are already formed before r=25 R$_*$ and the v 0−2 and v 1−2 lines before r=18 R$_*$ respectively. For model W64 strong NLTE effects in the lines will be expected if the formation of the line is not finished before r=18 R$_*$.

5.2 Formation depth of lines

Consequently, to investigate in which regions of the stellar atmosphere the formation of the lines are completed we have plotted the flux of selected characteristic rays (defined by the impact parameter p), which gives an insight at different stellar radii.

Fig. 3 shows such plots for model W64 and W69. For model W64 one can see that the v 0−2 line flux is already completely build up to r=18 R$_*$ (contribution to flux ~ 3 orders of magnitude smaller than final flux) whereas the v 0−1 and v 1−2 lines are completed around r=25 R$_*$. According to the results of Sec. 5.1 one can conclude all lines to be mainly LTE-lines apart from small NLTE effects in v 0−1 and v 1−2. However the situation is completely different for model W69: only the line v 0−2 is completed around r=18 R$_*$ in the LTE-region, whereas the other line fluxes still get big contributions from $r > 25$ R$_*$ and are therefore strongly influenced by NLTE effects. The lines are completed at very different radii in the atmosphere: v 1−2 is build around r=60 R$_*$ whereas v 0−1 still gets contributions to the line flux of the P-Cygni emission component coming from r=1500 R$_*$.

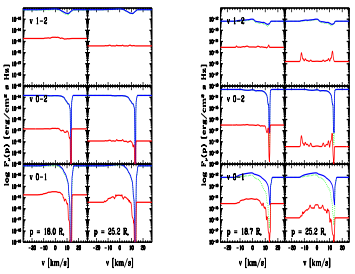

Fig. 3: Spectral flux contribution from chosen radius (given by impact parameter p) (red), flux integrated up to this radius (green) and the final line profile (blue) for R-branch transition R1 for all transitions v 0−1, v 0−2 and v 1−2 in W64 (left) and W69 (right).

5.3 Flux profiles

Fig. 4 depicts model W64 and the calculated line profiles for the R-branch transitions R1, R14, and R25. A comparison to profiles resulting from pure LTE-calculations (dashed) shows that in fact all lines can be well fitted by LTE-lines, as expected. Small deviations in the fundamental line are due to the minor NLTE effects in this transition. All lines have a more or less pronounced P-Cygni profile, as expected for expanding atmospheres. The emission component is most pronounced in v 0−1, which is due to its bigger oscillator strength and higher number density.

The first overtone represents a good example to explain the inner parts of the shell, because this line is formed up to r=18 R$_*$ (see Sec. 5.2). One can see two absorption dips at $10 - 14$ km/s (A1) and around -4 km/s (A2). Due to the formation depth and the velocity position of the dips A1 must originate from the two shocks at 8 R$_*$ and 16 R$_*$ whereas A2 is formed around the newly rising shock at 2 R$_*$. The fundamental line as well as the v 1−2 transition show the same results, however the A2 component gets filled by the emission component of the P-Cygni profile formed in the shell at r$\geq$ 10 R$_*$.

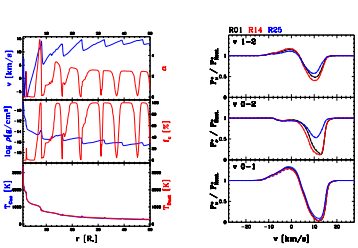

Fig. 4: **Left:** radial structure of model W64: upper panel: wind velocity v, radiative acceleration on dust α; middle panel: density ρ, degree of dust condensation f_c; lower panel: temperature of gas T_{gas} and of dust T_{dust}. **Right:** Resulting v 0−1, v 0−2, and v 1−2 band lines for $J = 0$ (black), 13 (red) and 24 (blue) in comparison to pure LTE-profiles (dashed in fitting colours).

Model W69 (Fig. 5) shows strong deviations from LTE for the v 0−1 and v 1−2 transitions, whereas the v 0−2 transition is mainly in LTE as expected. Although models W64 and W69 have similar hydrodynamical conditions in the shell, the latter leads to stronger P-Cygni emission components in the fundamental and v 1−2 transition. This is caused by the radiation field of the hotter star (see Tab. 1), which results in higher number densities by a factor of 100 to 1000 for the v=1 and v=2 bands in the outer regions r> 50 R_*.

Again the first overtone is a good example to analyze the inner parts of the shell due to the formation depth of the line (Sec. 5.2). One can see three absorption dips at $10 - 14$ km/s (A1), around $2 - 4$ km/s (A2) and at -4 km/s (A3), which must originate from r=1-18 R_*. Contributions to A1 can only originate from the two shocks at 7 R_* and 15 R_*, A2 must come from one wide absorption around the shock at 7 R_*, whereas A3 is formed around the first shock at 2 R_*. The emission component between A2 and A3 arises from the pre-shocked region at r=7-10 R_*.

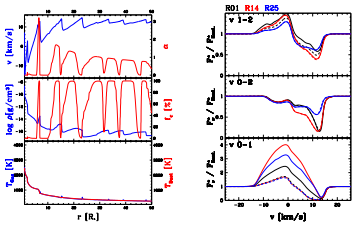

Fig. 5: Same as Fig. 4 but for model W69.

Assuming *all vibrational levels to be populated in LTE* Winters et al. 2000b calculated the fundamental and first overtone of CO using W64 at a different instant of time as one of their input models. For comparison we calculated the same model assuming *NLTE for all bands* (Fig. 6). Obviously our model profiles are close to theirs, but one can note that the observed profiles are reproduced even better with our results.

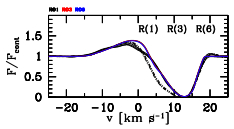

Fig. 6: Comparison between line profiles of our code (coloured lines) to calculated (dotted) and observed (dashed) profiles of Winters et al. 2000b.

6 Summary and outlook

We presented CO-line calculations for two hydrodynamical input models (W64, W69) which differ only in initial temperature. The code is performing detailed radiative transfer calculations of a 90 level CO-model-molecule (3 vibrational bands with 30 rotational levels each) under NLTE conditions in the awkward cool conditions of LPV atmospheres.

Analyzing the b-factors and the formation depth of the lines we concluded that model W64 is mainly leading to LTE-lines whereas the resulting lines for the hotter model W69 are strongly influenced by NLTE-effects. We discussed the detailed structure of the line profiles and gave an insight on how the hydrodynamic models leave their fingerprints on the profiles. Furthermore the comparison of our work with Winters et al. 2000b showed an excellent agreement of the line profiles with the observed profiles.

Presently work is in progress to model various permitted and forbidden metal lines with our code (see also poster contribution by Richter et al. "NLTE Modeling of Fe II and [Fe II] lines in the shocked atmospheres of M Miras"). The observations of M-type Mira stars from Richter & Wood 2001 should be explained to pin down detailed hydro- and thermodynamical conditions of the shocked layers near the photosphere and therewith obtain the barely known conditions of the dust-forming layers of Mira stars.

Acknowledgement:
We wish to thank Dr. A.B.C. Patzer for her helpful advice and fruitful discussions. This work was partly supported by the *Deutsche Forschungsgemeinschaft, DFG* project number SE 420/21-1.

References

Chakerian, C., Tipping, R.H.: 1983, J Molec. Spec. **99**, 431
Fleischer, A.J., Gauger, A., Sedlmayr, E.: 1992, A&A **266**, 321
Mihalas, D., Kunasz, P.B., Hummer, D.G.: 1975, ApJ **202**, 465
Puls, J., Herrero A.: 1988, A&A **204**, 219
Puls, J.: 1991, A&A **248**, 581
Rybicki, G.B.: 1971, NBS Spec. Pub. **332**, 87
Rybicki, G.B., Hummer, D.G.: 1991, A&A **245**, 171
Richtmyer, R.D., Morton, K.W.: 1967, John Wiley & Sons, New York, 2nd edition
Richter, He.: 1998, Diploma Thesis, Institut für Astronomie und Astrophysik, TU-Berlin
Richter, He., Wood, P.R.: 2001, A&A **369**, 1027
Winters, J.M., Le Bertre, T., Jeong, K.S., Helling, Ch., Sedlmayr, E.: 2000a, A&A **361**, 641
Winters, J.M., Keady, J.J., Gauger, A., Sada, P.V.: 2000b, A&A **359**, 651